Agrewale et al. 2019. *Int. J. Vehicle Structures & Systems*, 11(1), 39-46
ISSN: 0975-3060 (Print), 0975-3540 (Online)
doi: 10.4273/ijvss.11.1.09

International Journal of Vehicle Structures & Systems
Available online at www.maftree.org/eja

Investigation of Flow Induced Structural and Acoustic Behaviour of a Flat Solar Panel Mounted on a Mini Bus Roof Top

Mohammad Rafiq B. Agrewale[a] and R.S. Maurya[b]

Sardar Patel College of Engg., Mumbai, India
[a]Corresponding Author, Email: engg_rafiq@yahoo.co.in
[b]Email: r_maurya@spce.ac.in

ABSTRACT:

External fitting of a flat solar panel on a vehicle at its roof top changes the aerodynamics of flow around it. A local variation of pressure and velocity parameters around the solar panel at increasing speed and yaw angle may lead to structural instability and acoustic performance deterioration of the vehicle. Present paper addresses this issue numerically using ANSYS Fluent software. The investigation consists of three steps - flow analysis, structural analysis and acoustic analysis which focus more on flat solar panel and its supporting pillars. The vehicle speed is varied up to 100 kmph and yaw angle varied from 0° to 18°. The flow analysis reports pressure and velocity distribution, Structural analysis shows the deformation and stresses induced in panel and supporting pillars and Acoustic analysis captures the change in overall sound pressure level (OASPL) at front and rear location of the vehicle. The result of investigation shows no significant effect of flow induced effect on solar panel structure. Change in OASPL at front and rear end is observed to be marginal only.

KEYWORDS:

Mini bus; Solar panel; Co-efficient of drag and lift; Yaw angle; Structural; Acoustic analysis

CITATION:

M.R.B. Agrewale and R.S. Maurya. 2019. Investigation of Flow Induced Structural and Acoustic Behaviour of a Flat Solar Panel Mounted on a Mini Bus Roof Top, *Int. J. Vehicle Structures & Systems*, 11(1), 39-46. doi:10.4273/ijvss.11.1.09.

1. Introduction

In last two decades due to depleting reserve of fossil fuels and its impact on environment, have compelled researched to explore potential of other favourable sources of energy. Slowly maturing technologies to tap sun power as a source of energy has created hope to get rid of such problems. The automotive sector being a significant contributor to environmental issues, attracted researchers to carry out investigation in this direction. In recent years PV cell mounted vehicle on roof top has become very popular because of easy and convenient installation of solar panels. The mounting of solar panels on existing vehicle roof using fixtures alters the aerodynamic design of the vehicle which finally leads to the deterioration vehicle performance. The impact on performance can be depicted though the co-efficient of drag (C_D) and co-efficient of lift (C_L). Also any external fittings on vehicle body are expected to contribute to wind noise level. With mounting of flat solar panel on vehicle roof creates a cavity between roof and solar panel with sudden converging effect at front side and diverging effect at rear side. This may result in change in wind noise due to pressure difference.

Wind noise is measured through overall sound pressure level (OASPL). An assessment of this parameter is a customized activity which can be done either through experimentation or numerical investigation. Literature shows that many of the early investigations were on a simplified model of a vehicle known as Ahmed-body which was proposed by Ahmed et al [1]. He investigated the effect of rear slant angle from 0^o to 30^o on evolving wake flow structure behind Ahmed-body. Vino et al [2] investigated near end and far end wake formation around Ahmed-body. He observed sensitivity of drag coefficient with Reynolds number. The aerodynamic analysis of mini bus by Rodrigues et al [3] shows that small changes in vehicle geometry has been possible to achieve a reduction of almost 20% of drag co-efficient which results in fuel saving of about 10%. Mohamed et al [4] investigated different cases of bus design with consideration of front and rear curvature and observed that add-on gives reduction of drag up to 14%. Wang et al [5] carried out aerodynamic drag measurement by using filament method and laser flow visualization technique. This study provided foundation for styling optimization of a minibus.

Thorat and Rao [6] showed that slight modification in exterior bus design and frontal area with improved aesthetic, drag can be reduced significantly. An investigation of changing aerodynamics of a bus with small alteration such as boat end extension, panel and spoiler at rear side was done by Patil et al [7]. It was concluded that a drag reduction of about 20 to 30% is possible. Past, present and future use of solar energy, related issues, influencing parameters and modelling of solar car was reviewed by Singh et al [8]. In an experimental and numerical investigation of a hybrid

solar-bio-diesel car, Allgood [9] did wind tunnel test. He developed an optimum 2D shape of a car which had minimum drag co-efficient characteristics. Using COSMOS Flo-Works as numerical tool, Muhammad [10] investigated design of upper body structure for solar car and incorporated several changes such as frontal area, shape and material in the design and concluded that these are important parameters of design for better performance. Augenberges [11] carried out an aerodynamics optimization study of a solar powered race car using wind tunnel. He included the effect of parameters like - angle of attack, ride height, wheel fairing length, surface finish, sealing and rear view mirror in his study and optimized them for lower drag and better stability. Wolf-Heinrich Hucho [12] investigated the effect of yaw angle on vehicle drag on various commercial vehicles. He concluded that the drag co-efficient at zero yaw angle is equivalent to driving in still air which gives insufficient indication of aerodynamic characteristics in real operation, where the tangential force co-efficient due to yaw must be taken into account.

Bayraktar et al [13] explained experimental and computational investigation of external aerodynamics of Ahmed-body using various back angles and yaw angles up to ± 15 degrees. Singh et al. [14] performed numerical investigation on crosswind aerodynamics and its effect on the stability of a passenger car. The result shows that the drag co-efficient, lift coefficient and the yaw moment increases as the crosswind velocity increases. Howell [15] discussed the effect of various parameters on the drag rise with yaw for a range of different types of vehicle. The increase of drag with yaw is shown to be essentially induced drag, which is strongly dependent on both side force and lift. Lopes [16] studied the aerodynamic drag of a vehicle and trailer combination in yaw conditions. The result shows that the forces and moments change significantly at large yaw angles, and that zero yaw angle testing may be insufficient to predict the real world aerodynamics performance. Agrewale and Maurya [17] performed numerical investigation of evolving flow structure around Ahmed-body mounted with solar panel of different configuration which shows that shape of solar panel play significant role to improve fuel economy and vehicle performance. Also they have discussed the effect on vehicle performance with variation of rear slant angle and vehicle speed.

Mathew et al [18] investigated solar panel supporting structure subjected to wind force considering different wind zone and parameters. Naik et al. [19] performed analysis and optimization solar panel supporting structures using FEM under different loading conditions. Jakubec et al. [20] performed coupled CFD-structural analysis of solar panel parking spot considering horizontal direction of wind with two wind intensities. Mihailidas et al. [21] carried out analysis of solar panel support structures using CFD tool with different wind directions. They concluded that even fixed solar array support structures have sophisticated design, which needs to be analysed and often improved in order to withstand the wind load. In a review paper, George [22] presented aero-acoustic sources on automobiles and discussed about the state of experimental data, analysis method and noise reduction principles along with correlation to predict external fluctuating pressure. NurulMurad et al. [23] performed a CFD analysis of vehicle's A-pillar aero-acoustics.

He observed that extra turbulence was generated due to the A-pillar causing aerodynamic noise in the A-pillar region. Mukkamala et al. [24] investigated the effect of external rear view mirrors of a premium sedan on the sound pressure level at the A, B and C pillars using large eddy simulation. In a computational work, Oettle [25] assessed buffeting and broadband noise generated by a vehicle sunroof with different orientation of deflector. He showed that a meshed deflector at the front edge of sunroof reduces the sound pressure level. Erik Johansson [26] performed aero-acoustic study on the roof-bar of a truck using CFD with consideration of different turbulence model. It can be concluded that a significant contribution has been made by researchers to understand the flow dynamics of solar panel mounted vehicle. Few works are observed on solar panel support structures also, but most of them are dedicated to static condition (fixed to ground) only. Solar panel structure mounted on vehicle roof top work under several dynamic conditions and more prone to fail. Few works are observed on aero-acoustic performance of the vehicle. Present investigation aims to carryout investigation in this direction.

2. Problem definition

A large number of city vehicles can be easily altered to a partial solar powered vehicle without large investment which may significantly help this world to be greener. Unfortunately, there are no documented guidelines for the designers to suggest alteration without compromising significant vehicle performance. A systematic assessment of aerodynamic performance and its effect on mounted solar panel is a need of time which would help designer to recommend fitment of roof top solar panels. To investigate, a mini bus of size 6.5m length, 2.6m width and 3.8m height with roof top dimension of 5.6m length and 2.3m width flat solar panel, mounted at 150mm height is selected for investigation. The solar panel is mounted on mini bus using six vertical cylindrical supporting pillars of 100mm diameter each as a fixed joint as shown in Fig. 1. The fitting of solar panel is expected to alter the flow and acoustics of the vehicle.

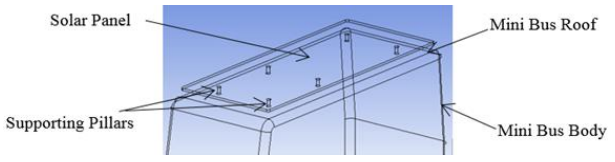

Fig. 1: Flat solar panel mounted on mini bus model

The objective of present work is to perform preliminary structural and acoustic analysis of flat solar panel mounted mini bus model under variable vehicle speed (60, 80 and 100kmph). Also, it is proposed to investigate the effect of yaw angle variation (6^o, 12^o and 18^o) at a constant speed. Fig. 2 shows a schematic diagram of the situation. An assessment of impact of

these parameters would help designer to take significant decision related to solar panel fixing on vehicle roof top.

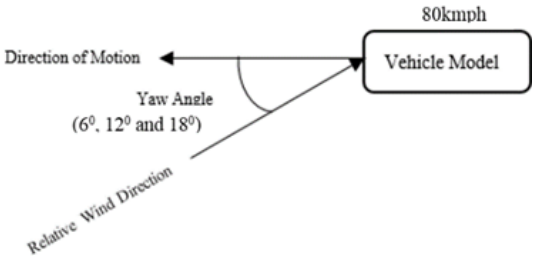

Fig. 2: Illustration of yaw angle variation

3. Flow analysis of solar panel mounted on vehicle roof top

A flat solar panel mounted on mini bus roof top supported by six rigid supports, provides scope for air flow to establish a specific flow structure around the panel while vehicle is in motion. A big difference of pressure between lower and top surface of the solar panel has potential to destroy the arrangement. In order to get insight of flow pattern developing around it, a flow analysis is presented. The flow around solar panel mounted vehicle is assumed to be three dimensional Newtonian, incompressible, isothermal and steady without any external energy interaction. Pressure gradient, viscous and inertial forces are main driving force. The presence of wake behind vehicle is common which influence the momentum equation. The body force can be completely neglected. The governing equations of flow are,

$$\frac{\partial u}{\partial x}+\frac{\partial v}{\partial y}+\frac{\partial w}{\partial z}=0 \quad (1)$$

$$-\frac{\partial p}{\partial x}+\mu\left(\frac{\partial^2 u}{\partial x^2}+\frac{\partial^2 u}{\partial y^2}+\frac{\partial^2 u}{\partial z^2}\right)=\rho\left(\frac{\partial u}{\partial t}+u\frac{\partial u}{\partial x}+v\frac{\partial u}{\partial y}+w\frac{\partial u}{\partial z}\right)$$

$$-\frac{\partial p}{\partial y}+\mu\left(\frac{\partial^2 v}{\partial x^2}+\frac{\partial^2 v}{\partial y^2}+\frac{\partial^2 v}{\partial z^2}\right)=\rho\left(\frac{\partial v}{\partial t}+u\frac{\partial v}{\partial x}+v\frac{\partial v}{\partial y}+w\frac{\partial v}{\partial z}\right)$$

$$-\frac{\partial p}{\partial z}+\mu\left(\frac{\partial^2 w}{\partial x^2}+\frac{\partial^2 w}{\partial y^2}+\frac{\partial^2 w}{\partial z^2}\right)=\rho\left(\frac{\partial w}{\partial t}+u\frac{\partial w}{\partial x}+v\frac{\partial w}{\partial y}+w\frac{\partial w}{\partial z}\right) \quad (2)$$

Transient terms are retained here to update velocity field under pseudo timing.

To model the turbulence arising in the present problem, with reference to Bengt Andersson et al [27], realizable turbulent kinetic energy- dissipation model is used as,

$$\frac{\partial}{\partial t}(\rho k)+\frac{\partial}{\partial x_j}(\rho k u_j)=\frac{\partial}{\partial x_j}\left[\left(\mu+\frac{\mu_t}{\sigma_k}\right)\frac{\partial k}{\partial x_j}\right]+G_k+G_b-\rho\epsilon-Y_M+S_k \quad (3)$$

Where,

G_k - Generation of turbulent kinetic energy, G_b - Generation of turbulent kinetic energy due to buoyancy, Y_M - Fluctuation dilation for compressible flows, S_k - Modulus of deformation tensor in kinetic energy, μ_t - Turbulent viscosity. The dissipation (ε) transport equation:

$$\frac{\partial}{\partial t}(\rho\epsilon)+\frac{\partial}{\partial x_j}(\rho\epsilon u_j)=\frac{\partial}{\partial x_j}\left[\left(\mu+\frac{\mu_t}{\sigma_\epsilon}\right)\frac{\partial \epsilon}{\partial x_j}\right]+\rho C_1 S_\epsilon-\rho C_2\frac{\epsilon^2}{k+\sqrt{\nu\epsilon}}+C_{1\epsilon}\frac{\epsilon}{k}C_{3\epsilon}G_b+S_\epsilon \quad (4)$$

Where $C_{1\epsilon}=1.44$, $C_{2\epsilon}=1.9$, $\sigma_k=1.0$, $\sigma_\epsilon=1.2$ are the coefficients of the model.

With a roof top solar panel, a vehicle moving at different speeds is expected to create a 3D turbulent flow field with a long vortex street. In order to capture the expected flow field, the computational domain of size (8L × 3.6B × 3.5H) is selected with 4% blockage ratio, 0.7 as aspect ratio and characteristic length of 6.5m where L, B and H are length, width and height of vehicle respectively. A half computational domain about longitudinal vertical plane is depicted in Fig. 3. The domain is meshed with sufficient fine size to capture all relevant physics. The domain and vehicle body are meshed using advance size function as proximity & curvature and patch confirming tetrahedrons method with an optimum cell size to capture all relevant details. The convergence criteria for residual of continuity, x, y and z are selected as 0.001. To take care of pressure-velocity coupling, pressure based solver with SIMPLE is chosen to carry out the investigation. The convective terms are interpolated by first by using for little initial iteration and then jumped to second order upwind schemes. Relaxation factors are appropriately chosen for smooth convergence of the case. The material properties of air at temperature 298K are chosen for investigation. Air approaches the computational domain with relative velocity 80kmph. Turbulent intensity and viscosity ratio are taken as 5% and 10 respectively.

The boundary conditions applicable to the problem under investigation are velocity inlet as per the speed of the vehicle, pressure outlet at far end of the vehicle, no-slip condition at the ground and body surface of the vehicle, and outflow at remaining sides. The velocity and pressure distribution shows the formation of flow structure occurring around the vehicle. At the front top of the vehicle above the solar panel flow is getting separated from the panel leading to a low pressure zone above the panel compared to the pressure developing between narrow gap of vehicle roof and solar panel. This pressure difference may significantly damage the panel structure. On downstream side near the end of plate length, the flow is observed to be getting attached again. After reattachment near the end of vehicle a bigger flow separation is observed behind the vehicle. The presence of vortices can be observed clearly. The drag experience by vehicle will be due to major form drag with a small contribution of friction drag. The average drag coefficient is found to be 0.439 at a speed of 80kmph. The variation of vehicle speed and its yaw angle leads to the variation in flow structure developing around it. Table 1 shows the effect of these parameters on C_D and C_L of the vehicle along with pressure difference ΔP developing across the flat solar panel. Higher pressure difference which is found to be increasing with increase in yaw angle has potential to deform the solar panel. The flow structure evolving around the vehicle is shown in Fig. 4 through pressure contour and velocity vector at speed of 80 kmph.

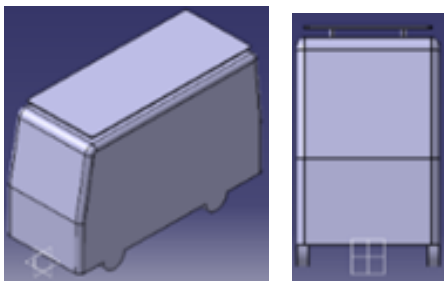

Fig. 3(a): Mini bus model

Fig. 3(b): Mesh around mini bus

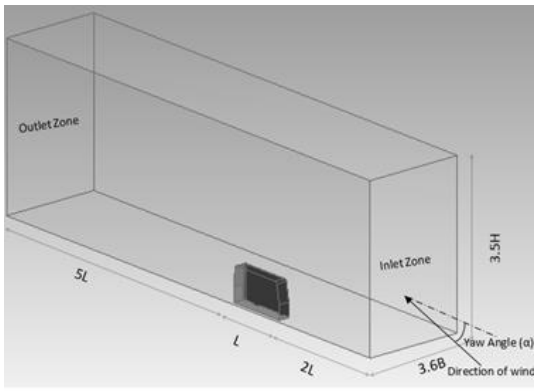

Fig. 3(c): Computational domain

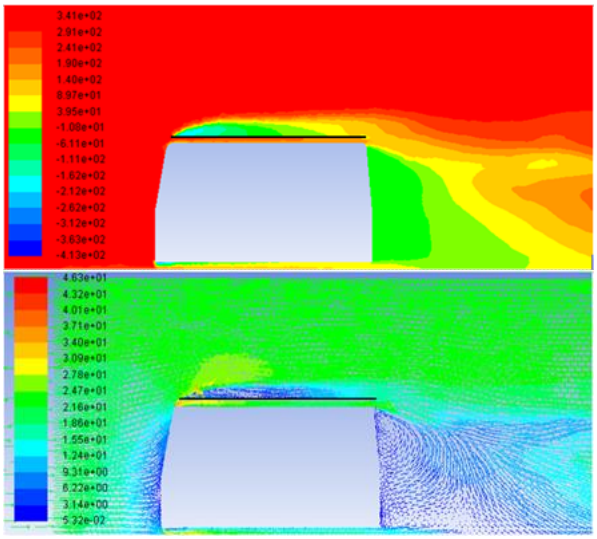

Fig. 4: Pressure and velocity distribution of flow around the model mini bus with flat solar panel

Table 1: Variation of drag and lift coefficients with change in speeds and yaw angles

Conditions		CD	CL	ΔP (N/m^2)
Change in speed (kmph)	60	0.44	0.006	382
	80	0.439	0.008	679
	100	0.438	0.006	1002
Change in yaw angle in degree at 80 kmph speed	6	0.573	0.055	908
	12	0.669	0.027	1157
	18	0.789	0.034	1423

4. Structural analysis

Under static condition pillars support the dead weight of the panel, but under dynamic condition, the front portion of panel and supporting pillars are subjected to high pressure difference as shown in Fig. 5 which may lead to damage to the panel and pillars. Therefore six pillars are not uniformly positioned. The middle pillar on both sides along the direction of flow are positioned (arbitrarily) closer to front one to take care of this non-uniform pressure load as shown in Fig. 6. The stress and deformation in elements are investigated under the variation of speed at 60, 80 and 100kmph with zero-degree yaw angle. Further the effect of change in yaw angle (6°, 12° and 18°) at 80kmph is presented here.

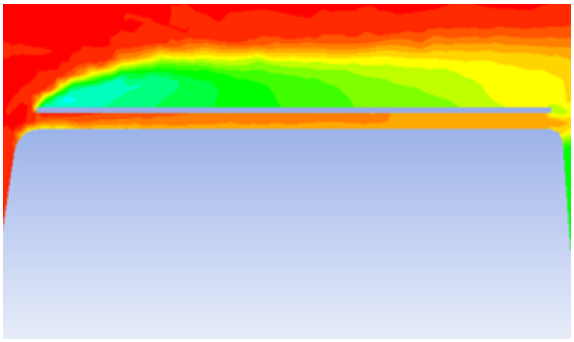

Fig. 5: Pressure variation around solar panel

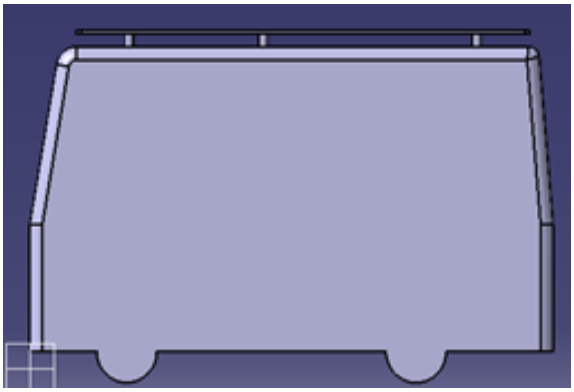

Fig. 6: Pillar positions for solar panel mounting

Fig. 7 shows the six pillars (p1, p2…..p6) of 100mm diameter each made up of steel and fixed to the roof frame. They support 600kg solar panel weight. Other than the dead weight, the pillars and panel are subjected to drag and lift forces as tabulated in Table 2. The work is executed through ANSYS Mechanical software. The solar panel and vehicle body are made up of silicon based material and structural steel respectively. The material properties are tabulated in Table 3.

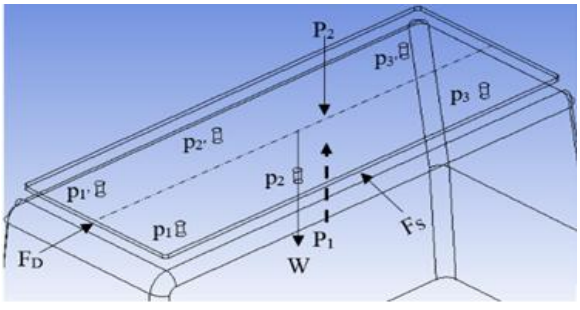

Fig. 7: Six pillars supporting flat solar panel

Table 2: Structural loads

Conditions		F_D (N)	F_S (N)	ΔP (N/m^2)	W (N)
Change in speed (kmph)	60	16.43	3.17	382	6000
	80	28.01	5.40	679	6000
	100	42.51	8.17	1002	6000
Change in yaw angle in degree at 80 kmph speed	6	32.77	7.37	908	6000
	12	40.17	8.83	1157	6000
	18	46.80	10.39	1423	6000

Table 3: Material properties

Parameter	Solar panel material	Vehicle body and pillars
Density	2270 kg/m^3	7850 kg/m^3
Young's Modulus	66300 MPa	2×10^5 MPa
Poison ratio	0.15	0.3
Tensile yield strength	45 MPa	250 MPa

4.1 Solar panel

At a zero-degree yaw angle, the speed of vehicle is varied to 60, 80 and 100kmph. The total deformation and induced equivalent stress on solar panel are depicted through contours in Fig. 8. The variation of total deformation and equivalent stress with speed is shown in Fig. 9. They are observed to be increasing with speed and have maximum value in between pillar p2 and p3. This can be attributed to bigger span between support and differential pressure developing across the panel. The magnitude of deformation and stresses are not of very high order from material failure point of view. The yaw angle is varied to 6^o, 12^o and 18^o at speed of 80kmph. The total deformation and induced equivalent stress on solar panel is shown in Fig. 10.

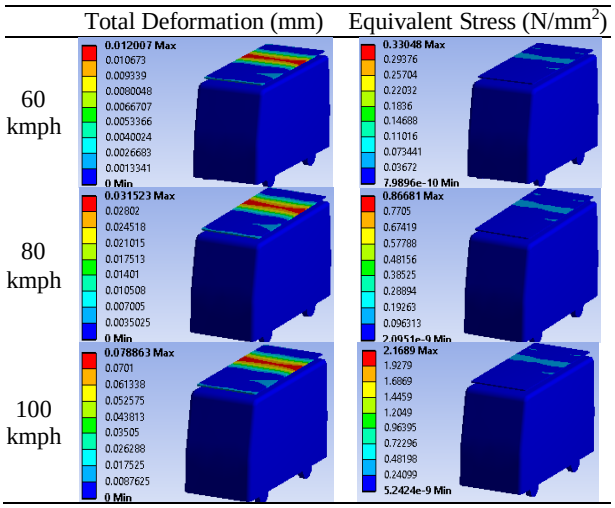

Fig. 8: Contour of deformation and stresses at different speed

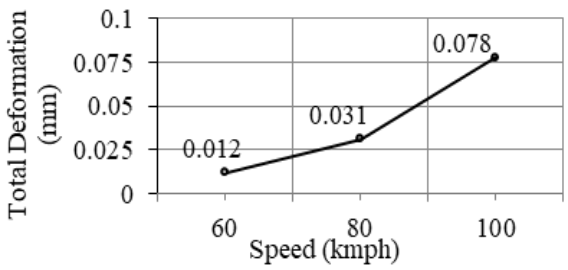

Fig. 9(a): Effect of speed on deformation

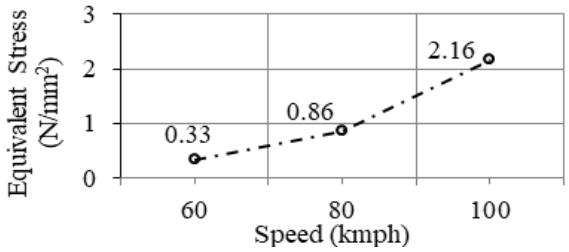

Fig. 9(b): Effect of speed on stress

Although the deformation and stress are can be observed to increase with change in yaw angles but magnitude of variation is so small that it can be neglected for any significant damage to solar panel. The maximum deformation is observed near rear pillar side due to more effect of turbulence. This is due to larger span between second and rear pillar support and bigger pressure difference across panel at this location.

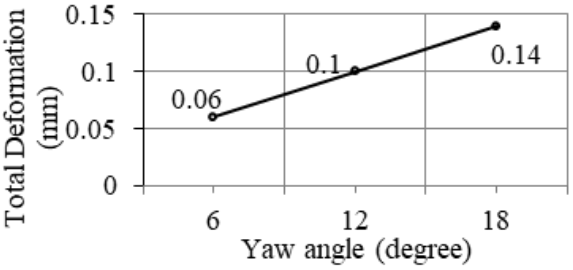

Fig. 10(a): Deformation variation in solar panel with respect to yaw angle

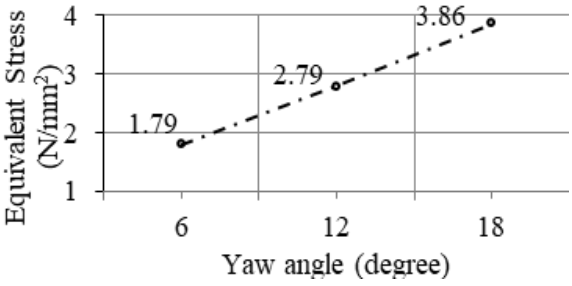

Fig. 10(b): Stress variation in solar panel with respect to yaw angle

4.2. Supporting pillars

Six pillars supporting the solar panel is expected to deform under aerodynamic effect with variable speed of the vehicle. The vehicle speed is varied from 60, 80 and 100 kmph at zero degree yaw angle. The simulation results in the form of total deformation and induced equivalent stress in supporting pillars are shown in Fig. 11. The result shows that the deformation is negligible as 0.0001 mm at low speed and increases up to 0.0009 mm with speed. The equivalent stress also shows similar trends on varying the speed. Its maximum observed value is on p3 which is 2.16 MPa. It is marginal as compared to yield stress of the material. This indicates the supporting members are strong enough to withstand under given loading condition without any failure.

On varying yaw angle from 6 to 18 degree at a speed of 80kmph, the contours of total deformation and equivalent stress developing on supporting pillars are shown in Fig. 12. The maximum deformation and equivalent stress is observed to be 0.0017 mm and 3.86 MPa respectively. They are visible on pillar p3 where

solar panel rests. The magnitude of maximum deformation is not very significant to cause any damage to solar panel. The maximum equivalent stress is also much below the yield strength value of the material of pillars. This indicates the supporting members are strong enough to withstand the deformation and stresses caused by change in yaw angle. The overall preliminary structure analysis shows that the deformation in solar panel and supporting pillars are low with consideration of change in speed and yaw angle.

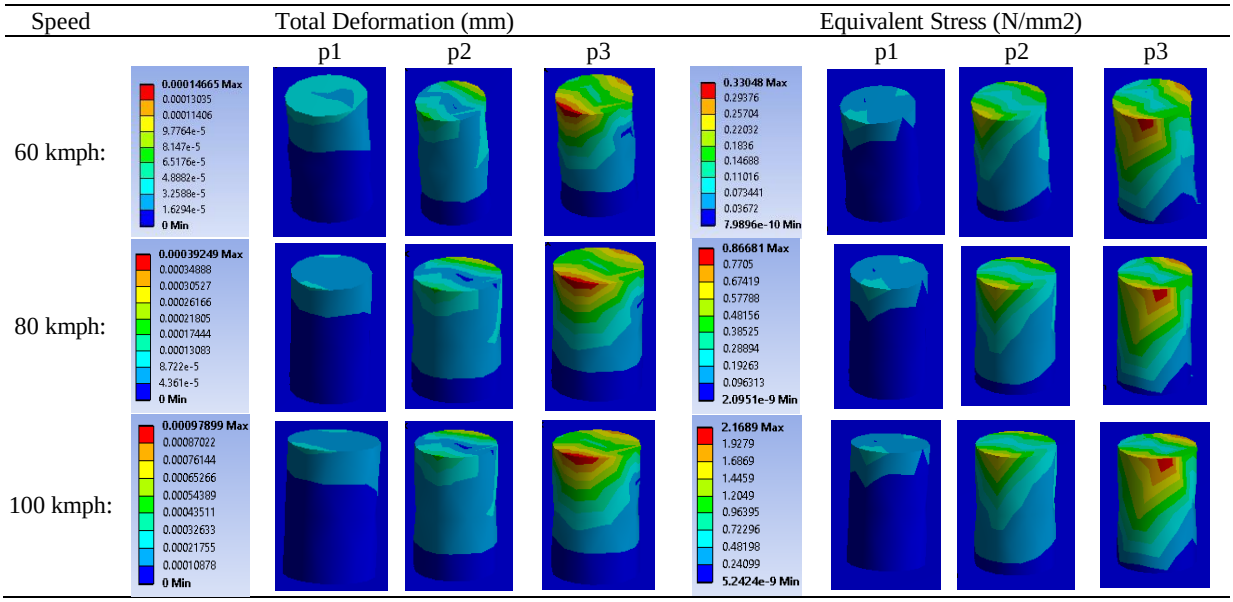

Fig. 11: Effect of speed on total deformation and equivalent stresses

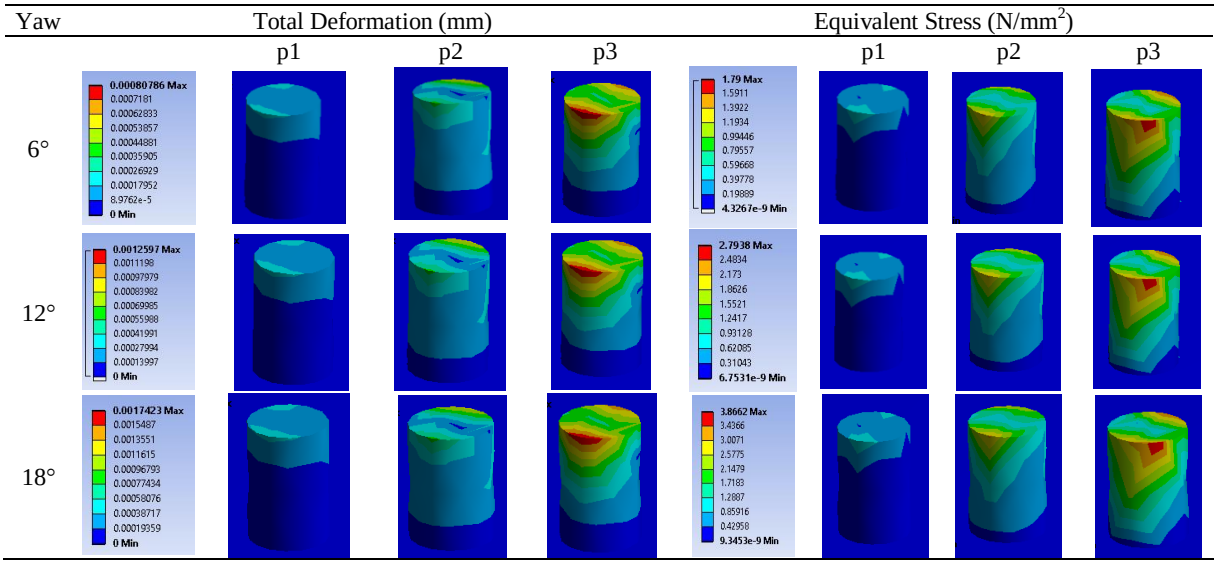

Fig. 12: Effect of yaw angle on total deformation and equivalent stresses

5. Acoustic analysis

The flow analysis shows a significant variation of pressure around the solar panel which may create pressure induced acoustic. In order to investigate this effect a numerical acoustic analysis is presented in this section. This analysis measures overall sound pressure level (OASPL). In present investigation two receivers- one at front side roof and other at rear side roof, are used to measure OASPL as shown in Fig. 13. The co-ordinates of receivers are specified in Table 4. The acoustic analysis is executed with turbulence model-LES with sub grid (Smagorinsky-Lilly). The boundary and operating conditions are listed in Table 5 and solver execution set-up is given in Table 6. OASPL received through receiver 1 and receiver 2 is shown in Table 7. The acoustic investigation shows a small change in OASPL for vehicle with solar panel mounted condition compared to without solar panel mounting.

Table 4: Co-ordinates of receivers

Position of receivers	Co-ordinates of receivers		
	x	y	z
Front side roof	0.578	3.8	0
Rear side roof	6.202	3.8	0

Table 5: Boundary conditions and operating conditions

Inlet velocity	80kmph
Pressure outlet	Atmospheric
Far - field density	1.225kg/m^3
Far - field sound speed	340m/s

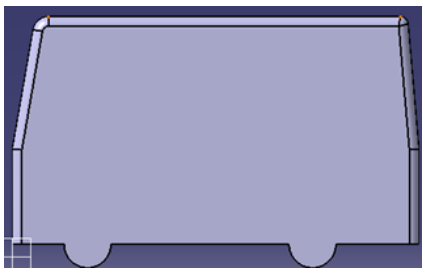

Fig. 13(a): Without solar panel

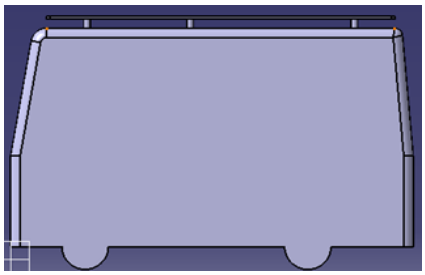

Fig. 13(b): With flat solar panel

Fig. 13: Mini bus model with receivers

Table 6: Solver setting for acoustic analysis

Parameter	Description
Scheme	SIMPLEC
Gradient	Green-Gauss Cell Based
Pressure	Standard
Momentum	Second order upwind
Transient Formulation	Bounded second order implicit
Time Step	0.0001s

An increase of about 4.1dB at receiver 1 and a decrease around 7.3dB at receiver 2 observed at zero degree yaw angle. Increase in OASPL at receiver 1 may be attributed to high pressure formed at front portion of vehicle structure roof and solar panel which is due to converging effect between roof and solar panel. The formation of low pressure wake region near receiver 2 may be the reason for decrease of OASPL. Also it is observed that as yaw angle changes, the OASPL gets affected. The OASPL increases with increase in yaw angle at receiver 2, whereas at receiver 1, the OASPL decreases with increase in yaw angle. This is because of impact of lateral and longitudinal air resistance components on vehicle due to yaw angle. The peak OASPL is observed at 18^o yaw angle.

Table 7: Receiver's data

Vehicle Condition	Yaw angle (degree)	OASPL (dB) Receiver 1	OASPL (dB) Receiver 2
Without solar panel	0	124.1	129.9
With flat solar panel	0	128.2	122.6
	6	120.6	126.17
	12	115.7	128.7

6. Conclusions

The investigation of possible structural changes in solar panel and its support caused by flow around the vehicle is performed successfully. Acoustic changes induced by flow are also investigated at two key locations. The structural deformation and equivalent stresses induced in solar panel and its supporting pillars due to solar panel mounting is not very serious from structural safety point of view for the cases where vehicle speed is maintained up to 100 kmph. Effect of yaw angle variation up to 18^o from direction of vehicle is also not significant. Flat panel mounting will induce a small increase in OASPL on the front side and reduction on the rear side of the panel. Yaw angle effect on OASPL is also marginal.

REFERENCES:

[1] S. Ahmed, G. Ramm and G. Faltin. 1984. Some salient features of the time-averaged ground vehicle wake, *SAE Technical Paper 840300*. https://doi.org/10.4271/840300.

[2] G. Vino, S. Watkin, P. Mousley, J. Watmuff and S. Prasad. 2005. Flow structures in the near wake of Ahmed model, *J. Fluids and Structures*, 20(5), 673-695. https://doi.org/10.1016/j.jfluidstructs.2005.03.006.

[3] A. Rodrigues, A. Cervieri, L.C. Gertz and M.A. Telh. 2014. Aerodynamic analysis of a vehicle minibus, *SAE Technical Paper 2014-36-0327*. https://doi.org/10.4271/2014-36-0327.

[4] E.A. Mohamed, M.N. Radhwi, and A.F.A. Gawad. 2015. Computational investigation of aerodynamic characteristics and drag reduction of a bus model, *American J. Aerospace Engg.*, 2(1-1), 64-73.

[5] J. Wang, X. Hu, Y. Zhang and B. Yang. 2011. Research of aerodynamic characteristics about mini bus, *Applied Mech. and Material*, 97-98, 752-755.

[6] S. Thorat and G.A.P. Rao. 2011. Computational analysis of intercity bus with improved aesthetic and aerodynamic performance on Indian roads, *Int. J. Advance Engg. Tech.*, 2(3), 103-109.

[7] C.N. Patil, K.S. Shashishekar, A.K. Balasubramanian and S.V. Subbaramaiah. 2012. Aerodynamic study and drag co-efficient optimization of passenger vehicle, *Int. J. Engg. Research & Tech.*, 1(7), 1-9.

[8] R. Singh, M.K. Gaur and C.S. Malvi. 2012. Study of solar energy operated hybrid mild cars: A review, *Int. J. Scientific Engg., and Tech.*, 1(4), 139-148.

[9] N.A. Allgood. 2008. Aerodynamic optimization of a solar-bio-diesel hybrid vehicle, *American Inst. of Aero. and Astronautics*.

[10] S.B.A. Muhammad. 2010. *Upper Body Structure Design for Solar Car*, Thesis, University Malaysia Pahang.

[11] P.K. Augenberges. 2005. *Aerodynamics Optimization of Solar Power Race Car*, Thesis, Massachusetts Institute of Tech.

[12] H. Wolf-Heinrich (Eds.) 1987. *Aerodynamics of Road Vehicles - From Fluid Mechanics to Vehicle Engg*., Butterworth-Heinemann Ltd.

[13] I. Bayraktar, D. Landman and O. Baysal. 2001. Experimental and computational investigation of Ahmed body for ground vehicle aerodynamics, *SAE Technical Paper 2001-01-2742*. https://doi.org/10.4271/2001-01-2742.

[14] M.G. Singh, Q.H.N.A. Nassar and S.R.S. 2009. Numerical investigations on crosswind aerodynamics and its effect on the stability of a passenger car, *SAE Technical Paper 2009-26-0059*. https://doi.org/10.4271/2009-26-0059.

[15] J. Howell. 2015. Aerodynamic drag of passenger cars at yaw, *SAE Int. J. Asseng. Cars-Mech. Syst.*, 8(1). https://doi.org/10.4271/2015-01-1559

[16] Y. Lopes, M. Taylor, T. Lounsberry and G. Fadler. 2017. Aerodynamic drag of a vehicle and trailer combination in

yaw, *SAE Technical Paper 2017-01-1540*. https://doi.org/10.4271/2017-01-1540.

[17] M.R.B. Agrewale and R.S. Maurya. 2017. Numerical study of flow structure developed around Ahmed body with roof top solar panel of different geometric configurations, *Int. J. Automobile Engg. Research and Development*, 127-136.

[18] A. Mathew, B. Biju, N. Mathews and V. Pathapadu. 2013. Design and stability analysis of solar panel supporting structure subjected to wind force, *Int. J. Engg. Research & Tech.*, 2 (12), 559-565.

[19] R. Naik, V.B. Melmari and A. Adeppa. 2013. Analysis and optimization solar panel supporting structures using FEM, *Int. J. Engg. and Innovative Tech.*, 2(7), 25-36.

[20] J. Jakubec, J. Paulech, V. Kutis, E. Mojto and V. Goga. 2013. Coupled CFD-structural analysis of solar panel parking spot, *Transfer Inovacii- 28/2013*.

[21] A. Mihailidas, K. Panagiotidis and K. Agouridas. 2009. Analysis of solar panel support structures, *3rd ANSA & µETA Int. Conf.*, Halkidiki Greece.

[22] A.R. Goerge. 1990. Automobile aerodynamic noise, *SAE Technical Paper 900315*. https://doi.org/10.4271/900315.

[23] M. Nurul, N. Jamal, A. Firoz and W. Simon. 2013. Computational fluid dynamics study of vehicle A-pillar aero-acoustics, *Applied Acoustics*, 74(6), 882-896. https://doi.org/10.1016/j.apacoust.2012.12.011

[24] Y Mukkamala, S. Devabhaktuni and V.G. Rajkumar. 2016. Computational aero-acoustic modelling of external rear-view mirrors on a mid-sized sedan, *Noise & Vibration Worldwide*, 47(1-2), 7-16. https://doi.org/10.1177/0957456516655224.

[25] N. Oettle, M. Meskine, S. Senthooran and A. Bissell. 2015. A computational approach to assess buffeting and broadband noise generated by a vehicle sunroof, *SAE Int. J. Passeng. Cars-Mech. Syst*, 8(1). https://doi.org/10.4271/2015-01-1532

[26] E. Johansson. 2013. *Aeroacoustic Study on The Roofbar of a Truck using CFD*, Master Thesis, Chalmers University of Technology, Sweden.

[27] B. Andersson, R. Andersson, L. Hakansson, M. Mortensen, R. Sudiyo and B. Wachem. 2011. *Computational Fluid Dynamics for Engineers*, Cambridge University Press. https://doi.org/10.1017/CBO9781139093590